inorganics

MDPI

Article

A Partial Anion Disorder in $SrVO_2H$ Induced by Biaxial Tensile Strain

Morito Namba [1], Hiroshi Takatsu [1,*], Wataru Yoshimune [1], Aurélien Daniel [1,2], Shoichi Itoh [3], Takahito Terashima [4] and Hiroshi Kageyama [1,*]

1 Department of Energy and Hydrocarbon Chemistry, Graduate School of Engineering, Kyoto University, Nishikyo-ku, Kyoto 615-8510, Japan; namba.morito.55w@st.kyoto-u.ac.jp (M.N.); yoshimune.wataru@gmail.com (W.Y.); aurelien.daniel40295@gmail.com (A.D.)

2 École Supérieure d'Ingénieurs de Rennes (ESIR), Université de Rennes 1, Campus de Beaulieu, 263, Avenue du Général Leclerc, 35042 Rennes CEDEX, France

3 Department of Earth and Planetary Sciences, Kyoto University, Kitashirakawaoiwake-cho, Sakyo-ku, Kyoto 606-8502, Japan; itoh.shoichi.8a@kyoto-u.ac.jp

4 Department of Physics, Kyoto University, Kitashirakawa, Sakyo-ku, Kyoto 606-8502, Japan; terashim@scl.kyoto-u.ac.jp

* Correspondence: takatsu@scl.kyoto-u.ac.jp (H.T.); kage@scl.kyoto-u.ac.jp (H.K.); Tel.: +81-075-383-2513 (H.T.); +81-075-383-2506 (H.K.)

Received: 16 March 2020; Accepted: 6 April 2020; Published: 8 April 2020

Abstract: $SrVO_2H$, obtained by a topochemical reaction of $SrVO_3$ perovskite using CaH_2, is an anion-ordered phase with hydride anions exclusively at the apical site. In this study, we conducted a CaH_2 reduction of $SrVO_3$ thin films epitaxially grown on $KTaO_3$ (KTO) substrates. When reacted at 530 °C for 12 h, we observed an intermediate phase characterized by a smaller tetragonality of c/a = 0.96 (vs. c/a = 0.93 for $SrVO_2H$), while a longer reaction of 24 h resulted in the known phase of $SrVO_2H$. This fact suggests that the intermediate phase is a metastable state stabilized by applying tensile strain from the KTO substrate (1.4%). In addition, secondary ion mass spectrometry (SIMS) revealed that the intermediate phase has a hydrogen content close to that of $SrVO_2H$, suggesting a partially disordered anion arrangement. Such kinetic trapping of an intermediate state by biaxial epitaxial strain not only helps to acquire a new state of matter but also advances our understanding of topochemical reaction processes in extended solids.

Keywords: oxyhydrides; $SrVO_2H$; thin film; epitaxial strain; *cis*/*trans* configuration; order–disorder

1. Introduction

Mixed-anion compounds have been attracting a great deal of attention due to their potential applications such as photocatalysts, anionic conductors, and thermoelectric materials [1]. In terms of structural chemistry, what distinguishes mixed-anion compounds from simple oxides is a heteroleptic coordination environment around a metal centre, which induces new degrees of freedom including *cis* and *trans* geometries for the MO_4X_2 octahedron. For example, the perovskite oxynitrides AMO_2N (e.g., $SrNbO_2N$, $SrTaO_2N$ [2], and $BaTaO_2N$ [3]) are composed of only *cis*-MO_4N_2 octahedra, which occurs in order to maximize more covalent M d_π–N p_π bonds [2]. This local constraint gives rise to *correlated disorder* with various types of zigzag –M–N–M–N– chains assembled within the perovskite framework [4], as originally stated by Pauling for the structure of ice [5]. Other mixed-anion oxides such as $BaScO_2H$, prepared under high pressure, and $SrFeO_2F$, prepared by the fluorination of $SrFeO_2$, exhibit a *cis* preference, but only partially [6,7].

Local coordination geometry can also be directed by the *d*-electron count. The vanadium oxyhydride $SrVO_2H$ (V^{3+}; d^2) (Figure 1b), prepared by topochemical hydride reduction of perovskite

$SrVO_3$ (Figure 1a) contains only *trans*-VO_4H_2 octahedra, as triply degenerate t_{2g} states are lifted by the *trans*-structure, leading to a stable $(d_{xz/yz})^2(d_{xy})^0$ configuration [8] as shown in Figure 1d. The resulting fully anion-ordered structure of [SrH] and [VO_2] layers can be regarded as a half-filled $(d_{xz/yz})^2$ system. Hydride anions at the apical sites function as "π-blocker" ligands [9], making this oxyhydride a quasi-two-dimensional Mott insulator [10]. A partial *trans*-preference has been proposed for the 6H-type perovskite $BaVO_{3-x}H_x$ ($0.5 < x < 0.9$) where the *d*-electron count, *n*, is $1.5 < n < 1.9$ [11].

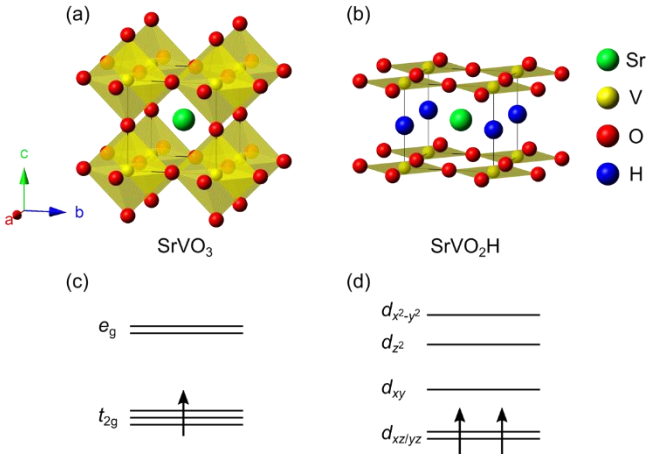

Figure 1. Crystal structures of (**a**) $SrVO_3$ (space group *Pm*–3*m*) and (**b**) $SrVO_2H$ (space group *P*4/*mmm*). Green, yellow, red and blue balls represent Sr, V, O and H atoms, respectively. The solid lines indicate unit cells. The crystal field splitting for (**c**) $SrVO_3$ and (**d**) $SrVO_2H$. Further splitting of $SrVO_2H$'s half-filled $(d_{xz/yz})^2$ band occurs due to on-site Columbic repulsion, leading to a Mott insulating ground state.

Transformation from *cis* to *trans* or vice versa is an important and challenging issue that may allow for tuning chemical and physical properties. As mentioned above, the TaO_4N_2 octahedra in $ATaO_2N$ are exclusively of *cis* configuration, but the short-range-ordered state with zigzag –M–N–M–N– chains is not polar (or ferroelectric), which is unfortunate given the more polarizable nature of nitride anions compared with oxide anions. However, the recent thin film study of $SrTaO_2N$ and its Ca-substituted solid solution has shown that the application of compressive biaxial strain from a $SrTiO_3$ (STO) substrate induces a partial transformation to *trans* [12,13], leading to ferroelectric behavior [12].

The present study addresses a case where *trans*-VO_4H_2 octahedra in $SrVO_2H$ are converted partially to *cis* coordination. It has been previously shown that $SrVO_2H$ thin films, under small compressive strain (−0.7%) from $SrTiO_3$ (001) (a = 3.905 Å) substrates have a fully anion-ordered phase (with 100% *trans*-coordination) [14], as in the bulk case [8]. Here, we applied tensile strain (1.4%) by using a $KTaO_3$ (001) substrate (KTO, a = 3.989 Å). While the reaction of the $SrVO_3$/KTO thin film with CaH_2 for 24 h gave the known $SrVO_2H$ phase, reacting it for 12 h gave rise to an intermediate state, which is potentially a partially anion-disordered $SrVO_2H$, with [$SrH_{1-x}O_x$] and [$VO_{2-x}H_x$] layers. We discuss the possible origin of the formation of the intermediate phase in view of the kinetics.

2. Results and Discussion

2.1. Low-Temperature Reduction of $SrVO_3$ Films

$SrVO_3$ films with a thickness of about 100 nm were grown on KTO substrates and were reacted with CaH_2 at 530 °C for 12 and 24 h, respectively. The lower reaction temperature compared to that of the powder samples (610 °C) [8] is due to a short anion diffusion path for thin films, as in the case of $SrVO_2H$/STO [14]. The reduced films were investigated using high-resolution X-ray diffraction (XRD). The out-of-plane θ–2θ XRD scans are shown in Figure 2a, along with the as-deposited film (i.e., before reduction). The 2θ peak at 47.4°, corresponding to c = 3.83 Å, can be assigned to the 002 reflection of

$SrVO_3$ (a = 3.841 Å for bulk [15]). Both reduced samples exhibited only 00l peaks, indicating a good orientation of the films along the c axis. For the 24h-reacted $SrVO_3$ film, the 002 peak is significantly shifted to a higher angle of 49.4° corresponding to c = 3.68 Å, which is close to that of bulk $SrVO_2H$ (c = 3.6671(3) Å [8]). Most remarkably, the 002 peak for the 12h-reacted film appears between these two peaks. This peak is absent in bulk [8] and thin film (on the STO substrate) [14] samples of reduced $SrVO_3$, suggesting the emergence of an intermediate phase. This intermediate phase could not be assigned simply as $SrVO_{3-\delta}$ with random anion vacancies, because the 00l peaks should appear at lower angles than for $SrVO_3$ [8,14]. The FWHM of the θ–2θ peaks for the film reacted for 12 h is broader than the film reacted for 24 h (Figure 2a), implying lower crystallinity and/or a certain compositional distribution. Note that epitaxial $SrVO_2H$ films cannot be obtained on an $(La_{0.3}Sr_{0.7})(Al_{0.65}Ta_{0.35})O_3$ (LSAT) substrate, which provides a compressive strain of −1.7% [14], and this was reproduced in our study (not shown). It is also reported that even small tensile strain from a $DyScO_3$ substrate (0.3%) destabilizes the $SrVO_2H$ phase [14].

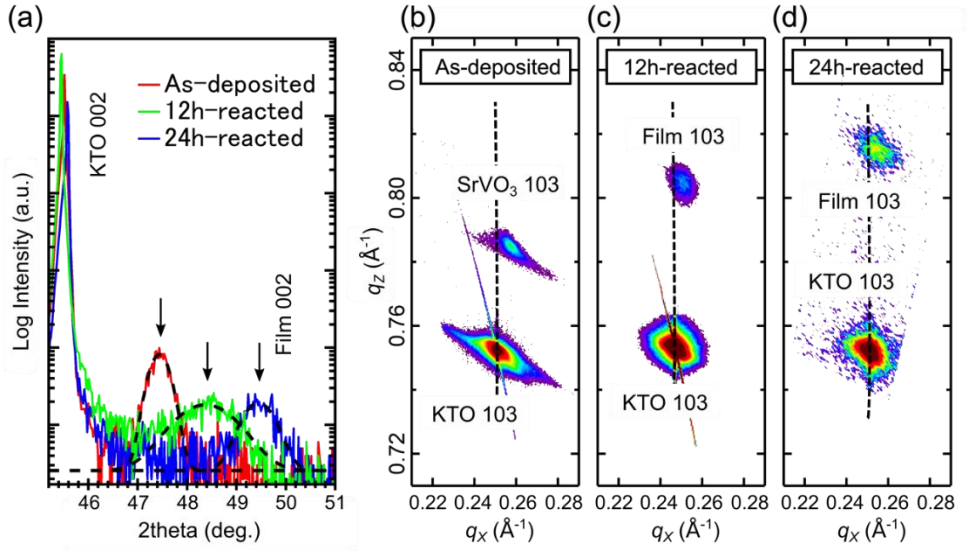

Figure 2. (**a**) XRD θ–2θ scans around the 002 peaks of the as-deposited, 12h-reacted, and 24h-reacted $SrVO_3$ thin films on the $KTaO_3$ substrates. The broken lines represent Gaussian fits. (**b**–**d**) RSM around the 103 reflections for the as-deposited (**b**), 12h-reacted (**c**), and 24h-reacted (**d**) $SrVO_3$ thin films.

2.2. Structural CharacterizatIon

To further investigate the crystal structures of the three films on the KTO substrates, XRD reciprocal space mapping (RSM) measurements were performed around the 103 reflection, and the results are shown in Figure 2b–d. The in-plane positions of the 103 reflections of the 12h- and 24h-reacted films are found to be near the q_x positions of the KTO substrates (shown by the dashed lines), suggesting that both films are grown almost coherently, unlike the as-deposited $SrVO_3$ film that is relatively relaxed. There was no domain formation or orientation change, which was often observed in strained films [16] or films after metal hydride treatments [17,18]. The estimated lattice parameters for the as-deposited $SrVO_3$ film are a = 3.85 Å and c = 3.83 Å, indicating a small tetragonal lattice distortion (c/a = 0.995) compared to the bulk (cubic; a = 3.841 Å [15]), although RSM showed a partial relaxation (Figure 2b). The cell constants (a = 3.95 Å and c = 3.68 Å) for the 24h-reacted film indicate that the reduced film is slightly under tension, compared with bulk $SrVO_2H$ (a = 3.9331(4) Å, c = 3.6671(3) Å) [8]. One can therefore presume that tensile strain has been continuously applied to the films via the KTO substrate throughout the whole reaction process from $SrVO_3$ to $SrVO_2H$. Note that even if the KTO substrate is reduced, the corresponding cell expansion and resulting effect on strain should be very small, as XRD data did not show any anomalies.

The hydride exchange was examined with secondary ion mass spectrometry (SIMS). We measured two areas (100×100 μm^2) of each film in order to investigate the hydrogen content and its distribution. Figure 3 shows the SIMS profiles of the ratio of secondary ion intensities ^{1}H/^{18}O for the films after 12 h and 24 h reduction. For both films, a high hydrogen signal was observed, with clear contrast at the boundary between the substrate and the film. The hydrogen signal in the KTO substrate is much smaller than the target films, though it is 10–100 times higher than the case of LSAT [19,20], which might reflect some reactivity with CaH_2. For the film reacted for 24 h (i.e., $SrVO_2H$), homogeneous hydrogen distribution is confirmed, with ^{1}H/^{18}O values at the two areas of 7.2 (2SD 0.5) (Figure 3, blue) and 7.5 (2SD 1.0). Most importantly, hydrogen is almost homogeneously distributed in the 12h-reacted film, with ^{1}H/^{18}O values of 7.4 (2SD 1.4) (Figure 3, red) and 8.2 (2SD 0.8), similarly to those of the 24h-reacted film. This result strongly suggests that the intermediate phase has roughly the same hydride concentration as $SrVO_2H$, though it might have some level of anion nonstoichiometry. This interpretation is supported by the close cell volumes (57.5 Å^3 and 57.4 Å^3 for 12h- and 24h-reacted films, respectively). The intermediate tetragonal phase is less anisotropic with a $c/a = 0.96$, compared to the 24h-reacted film and the bulk sample of $SrVO_2H$ with a $c/a = 0.93$.

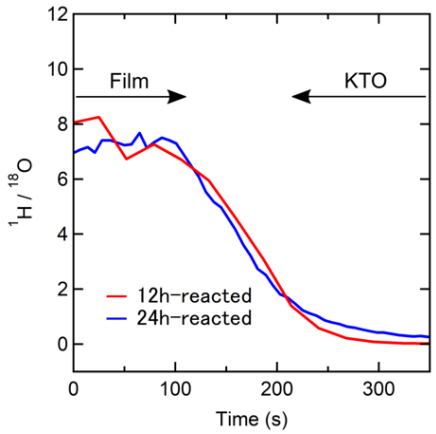

Figure 3. SIMS profiles of the $SrVO_3$ films on $KTaO_3$ substrates after CaH_2 treatment for 12 h and 24 h. Secondary ion intensity ratio of ^{1}H/^{18}O plotted with respect to sputtering time.

Since the anisotropic lattice parameter of bulk $SrVO_2H$ obviously arises from the full anion (H^-/O^{2-}) order, the most natural origin of the suppressed anisotropy for the intermediate phase would be a partial anti-site disorder, where the structure consists of alternating stacks of $[SrH_{1-x}O_x]$ and $[VO_{2-x}H_x]$ layers (where $0 < x < 1$). One can roughly estimate the degree of order $(1 - 3x/2)$ to be 0.57 for the 12h-reacted film ($c/a = 0.96$, $x = 0.29$) by simply interpolating the c/a value between the 'hypothetical' fully disordered cubic phase with $[SrH_{1/3}O_{2/3}]$ and $[VO_{4/3}H_{2/3}]$ layers ($c/a = 1$, $x = 2/3$), and the fully ordered one ($c/a = 0.93$, $x = 0$). The partial anti-site disorder in the intermediate phase indicates the presence of *cis*-VO_4H_2 octahedra (Figure 4b). The broad FWHM observed in the XRD profiles for the 12h-reacted film (Figure 2a) implies either a certain local variation in anion ordering or buckled $[VO_{2-x}H_x]$ layers as observed in Ln-doped $SrFeO_{2+\delta}$ [21]. Further studies are necessary to clarify the anion arrangement of this intermediate phase, using, e.g., linearly polarized X-ray absorption spectroscopy as utilized to determine *cis*/*trans*-TaO_4N_2 configuration in Ca-doped $SrTaO_2N$ [13].

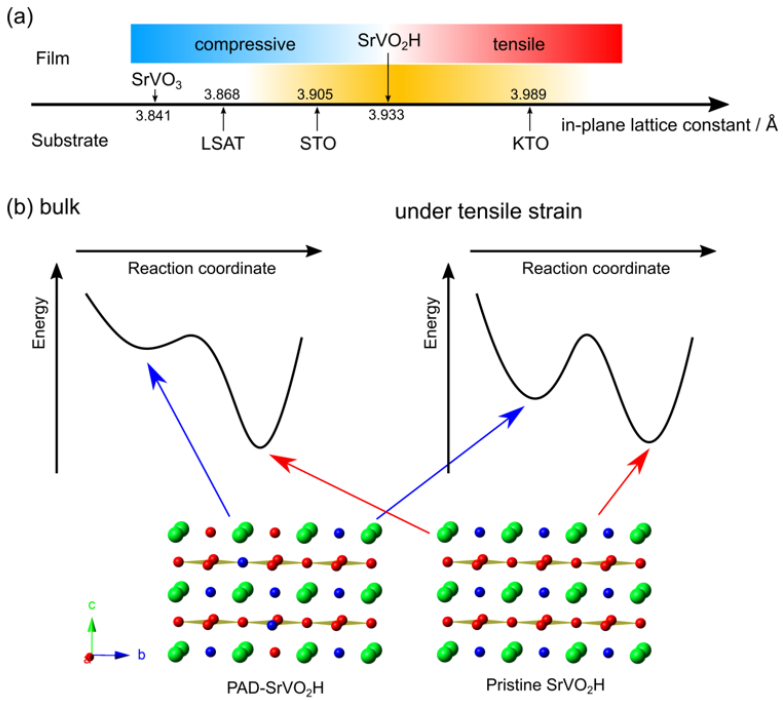

Figure 4. (**a**) In-plane lattice constants of $SrVO_3$, $SrVO_2H$ and substrates. The orange area shows the range where $SrVO_2H$ can be synthesized. (**b**) Energy diagrams with respect to the reaction coordinate for the reaction from (left) bulk $SrVO_3$ and (right) $SrVO_3$ thin film under tensile strain. Partially anion disordered (PAD) $SrVO_2H$ is a kinetically trapped transient state observed when tensile strain is applied (after 12 h reaction at 530 °C). A longer reaction (24 h) transforms this intermediate state to $SrVO_2H$ with complete anion order.

2.3. The Role of Tensile Strain

The previous bulk and thin film studies showed that $SrVO_2H$ with a fully anion-ordered (thus all *trans*) structure is a stoichiometric phase (or a line phase) [8,14]. A recent study showed that a small amount of Ti substitution (5%) of V is able to change anionic composition and crystal symmetry, leading to the cubic perovskite $SrV_{0.95}Ti_{0.05}O_{1.5}H_{1.5}$ (a = 3.888(1) Å) [22]. The present study demonstrates that an intermediate tetragonal phase appears when the $SrVO_3$ film on the KTO substrate reacts with CaH_2 in a short period of time (12 h), and its composition is roughly given by $SrVO_2H$. The structure is most likely a partially anion-disordered $SrVO_2H$ (PAD-$SrVO_2H$), thus having partial *cis*-geometry. Given the absence of such an intermediate phase in the case of the STO substrate with compressive strain [14], the application of tensile strain by the KTO substrate potentially plays a key role in stabilizing PAD-$SrVO_2H$ (Figure 4a).

Recall that a longer time treatment with CaH_2 (e.g., 24 h) resulted in the anion-ordered $SrVO_2H$ (Figure 1b). This fact strongly suggests that the partially disordered phase is a kinetically trapped transient state, shown in the reaction coordinate diagram in Figure 4b. In the bulk form, the energy of PAD-$SrVO_2H$'s state is rather high and the potential well of this state is shallow (meaning a low activation energy to the final phase of $SrVO_2H$) so that hydride reduction of $SrVO_3$ leads rapidly to the anion-ordered $SrVO_2H$ (Figure 4b, left). On the other hand, when tensile strain is applied, the PAD-$SrVO_2H$ state may be kinetically trapped if the strain can stabilize this state (Figure 4b, right), but the increase in the activation energy is not high enough to stop the further reaction from occurring at 530 °C. The origin is not clear, but the stabilization of PAD-$SrVO_2H$ by tensile strain might be rationalized from examples with other perovskites, where tensile strain tends to induce oxygen deficiencies (or hydride anions, in our case) at equatorial sites [23].

It is worth considering the reaction route from $SrVO_3$ to $SrVO_2H$, which involves H^-/O^{2-} exchange at the surface and hydride/oxide diffusion in the film [24]. In perovskites, oxide anion diffusion occurs

along the octahedral edge (the nearest-neighbor pathway). The involvement of the equatorial oxide anion can be easily understood by the low-temperature conversion from $SrFeO_3$ to $SrFeO_2$ via a $SrFeO_{2.5}$ intermediate [25]. Hopping of oxide anions (or oxygen vacancies) involving the equatorial site is also suggested in the layered perovskite oxide $Sr_3Fe_2O_{7-x}$ ($0 \leq x \leq 1$) [26]. The importance of nearest-neighbor anion hopping via octahedral edges has been pointed out for $BaTi(O,H)_3$ [27]. Accordingly, in our case H^-/O^{2-} anion migration predominantly takes place (via anion vacancies) along the $V(O,H)_6$ octahedral edge, rather than the next-nearest-neighbor hopping between the apical sites. If this is the case, when the H^-/O^{2-} exchange proceeds and the hydride content reaches (close to) 1, a partially anion-disordered phase with a composition close to $SrVO_2H$ will be formed, which is subsequently transformed into the fully anion-ordered $SrVO_2H$.

3. Materials and Methods

Epitaxial films of the $SrVO_3$ precursor with a thickness of ~100 nm were grown by using pulsed laser deposition on (001)-oriented KTO substrates. A target of the $Sr_2V_2O_7$ pellet, prepared at 800 °C in air, was ablated by a KrF excimer laser (λ = 248 nm) with an energy density of 0.6 J/cm^2 and 1 Hz repetition rate. The films were deposited at a substrate temperature of 700–750 °C under vacuum (~1×10^{-6} Pa). The $SrVO_3$ film obtained was embedded in 0.2 g of CaH_2 powder in a quartz tube, sealed under vacuum (<4×10^{-2} Pa), and then heated at 530 °C for 12 or 24 h. After these reactions, the residual CaH_2 and the resulting CaO byproducts on the surface of the films were removed by washing with anhydrous acetone. XRD measurements were performed at room temperature with a RigakuSmartLab diffractometer and a Cu Kα radiation (Rigaku, Akishima, Japan). SIMS measurements were performed for detecting hydrogen in the films using a Cameca ims-4f-E7 SIMS (Cameca, Gennevilliers France) at Kyoto University. The primary ion was $^{133}Cs^+$ ion, accelerated at 14.5 keV to obtain depth profiles at 100×100 μm^2 areas for each film.

4. Conclusions

We found the intermediate tetragonal phase between $SrVO_3$ perovskite and anion-ordered $SrVO_2H$ when the $SrVO_3$ thin film (epitaxially grown on the KTO substrate) was treated with CaH_2 for 12 h at 530 °C. XRD and SIMS results show that this intermediate phase is less anisotropic with c/a = 0.96 (vs. 0.93 in $SrVO_2H$) and similar hydrogen content, implying the formation of a partially anion-disordered phase of roughly anion stoichiometric $SrVO_2H$. Since a longer reaction time resulted in the known anion-ordered phase of $SrVO_2H$, this phase is considered an intermediate state, possibly stabilized by applying tensile strain from the KTO substrate. This phase, with partial *cis*-structure, is also rationalized when considering the reaction process from $SrVO_3$ to $SrVO_2H$, which should involve anion migration through the octahedral edge. Stabilization of such an intermediate state has been demonstrated in many systems tuned by various parameters. For example, high pressure and temperature can kinetically trap a metastable state of dichalcogenides, MnS_2, CuS_2, and ZnS_2 [28–30]. The metastable ordered state of a ternary alloy is discussed in terms of the kinetics of atomic species in crystallization [31]. In the present study, we suggest that strain engineering offers a useful strategy to kinetically trap metastable states. Despite numerous examples, topochemical reactions in extended solids have remained poorly understood. The present study sheds light on the underlying reaction mechanism.

Author Contributions: M.N., H.T., and H.K. conceived and designed the experiments; M.N., A.D., H.T., and T.T. conducted and performed thin film growth; M.N., H.T., and W.Y. performed XRD experiments; M.N., W.Y., and S.I. conducted SIMS experiments; M.N., H.T., W.Y., S.I., and H.K. analyzed data; M.N., H.T., and H.K. wrote the paper, with suggestions from other authors. All authors have read and agreed to the published version of the manuscript.

Funding: The research was funded by CREST Grant Number JPMJCR1421, and JSPS KAKENHI Grant Numbers 16H06439 and 17H04849.

Acknowledgments: We acknowledge Yoshinori Higashi for SIMS analyses at LPS lab at Kyoto University.

Conflicts of Interest: The authors declare no conflict of interest.

References

1. Kageyama, H.; Hayashi, K.; Maeda, K.; Attfield, J.P.; Hiroi, Z.; Rondinelli, J.M.; Poeppelmeier, K.R. Expanding frontiers in materials chemistry and physics with multiple anions. *Nat. Commun.* **2018**, *9*, 772. [CrossRef] [PubMed]
2. Yang, M.; Oró-Solé, J.; Rodgers, J.A.; Jorge, A.B.; Fuertes, A.; Attfield, J.P. Anion order in perovskite oxynitrides. *Nat. Chem.* **2011**, *3*, 47–52. [CrossRef] [PubMed]
3. Page, K.; Stoltzfus, M.W.; Kim, Y.I.; Proffen, T.; Woodward, P.M.; Cheetham, A.K.; Seshadri, R. Local atomic ordering in $BaTaO_2N$ studied by neutron pair distribution function analysis and density functional theory. *Chem. Mater.* **2007**, *19*, 4037–4042. [CrossRef]
4. Camp, P.J.; Fuertes, A.; Attfield, J.P. Subextensive entropies and open order in perovskite oxynitrides. *J. Am. Chem. Soc.* **2012**, *134*, 6762–6766. [CrossRef] [PubMed]
5. Pauling, L. The structure and entropy of ice and of other crystals with some randomness of atomic arrangement. *J. Am. Chem. Soc.* **1935**, *57*, 2680–2684. [CrossRef]
6. Goto, Y.; Tassel, C.; Noda, Y.; Hernandez, O.; Pickard, C.J.; Green, M.A.; Sakaebe, H.; Taguchi, N.; Uchimoto, Y.; Kobayashi, Y.; et al. Pressure-stabilized cubic perovskite oxyhydride $BaScO_2H$. *Inorg. Chem.* **2017**, *56*, 4840–4845. [CrossRef]
7. Blakely, C.K.; Davis, J.D.; Bruno, S.R.; Kraemer, S.K.; Zhu, M.; Ke, X.; Bi, W.; Alp, E.E.; Poltavets, V.V. Multistep synthesis of the $SrFeO_2F$ perovskite oxyfluoride via the $SrFeO_2$ infinite-layer intermediate. *J. Fluor. Chem.* **2014**, *159*, 8–14. [CrossRef]
8. Denis Romero, F.; Leach, A.; Möller, J.S.; Foronda, F.; Blundell, S.J.; Hayward, M.A. Strontium vanadium oxide-hydrides: "square-planar" two-electron phases. *Angew. Chem. Int. Ed.* **2014**, *53*, 7556–7559. [CrossRef] [PubMed]
9. Yamamoto, T.; Zeng, D.; Kawakami, T.; Arcisauskaite, V.; Yata, K.; Patino, M.A.; Izumo, N.; McGrady, J.E.; Kageyama, H.; Hayward, M.A. The role of π-blocking hydride ligands in a pressure-induced insulator-to-metal phase transition in $SrVO_2H$. *Nat. Commun.* **2017**, *8*, 1217. [CrossRef] [PubMed]
10. Wei, Y.; Gui, H.; Li, X.; Zhao, Z.; Zhao, Y.H.; Xie, W. The effect of hydrogen ordering on the electronic and magnetic properties of the strontium vanadium oxyhydride. *J. Phys. Condens. Matter* **2015**, *27*, 206001. [CrossRef] [PubMed]
11. Yamamoto, T.; Shitara, K.; Kitagawa, S.; Kuwabara, A.; Kuroe, M.; Ishida, K.; Ochi, M.; Kuroki, K.; Fujii, K.; Yashima, M.; et al. Selective hydride occupation in $BaVO_{3-x}H_x$ ($0.3 \leq x \leq 0.8$) with face and corner-shared octahedra. *Chem. Mater.* **2018**, *30*, 1566–1574. [CrossRef]
12. Oka, D.; Hirose, Y.; Kamisaka, H.; Fukumura, T.; Sasa, K.; Ishii, S.; Matsuzaki, H.; Sato, Y.; Ikuhara, Y.; Hasegawa, T. Possible ferroelectricity in perovskite oxynitride $SrTaO_2N$ epitaxial thin films. *Sci. Rep.* **2014**, *4*, 1–6. [CrossRef]
13. Oka, D.; Hirose, Y.; Matsui, F.; Kamisaka, H.; Oguchi, T.; Maejima, N.; Nishikawa, H.; Muro, T.; Hayashi, K.; Hasegawa, T. Strain engineering for anion arrangement in perovskite oxynitrides. *ACS Nano* **2017**, *11*, 3860–3866. [CrossRef] [PubMed]
14. Katayama, T.; Chikamatsu, A.; Yamada, K.; Shigematsu, K.; Onozuka, T.; Minohara, M.; Kumigashira, H.; Ikenaga, E.; Hasegawa, T. Epitaxial growth and electronic structure of oxyhydride $SrVO_2H$ thin films. *J. Appl. Phys.* **2016**, *120*, 085305. [CrossRef]
15. Rey, M.J.; Dehaudt, P.; Joubert, J.C.; Lambert-Andron, B.; Cyrot, M.; Cyrot-Lackmann, F. Preparation and structure of the compounds $SrVO_3$ and Sr_2VO_4. *J. Solid State Chem.* **1990**, *86*, 101–108. [CrossRef]
16. Folkman, C.M.; Baek, S.H.; Jang, H.W.; Eom, C.B.; Nelson, C.T.; Pan, X.Q.; Li, Y.L.; Chen, L.Q.; Kumar, A.; Gopalan, V.; et al. Stripe domain structure in epitaxial (001) $BiFeO_3$ thin films on orthorhombic $TbScO_3$ substrate. *Appl. Phys. Lett.* **2009**, *94*, 251911. [CrossRef]
17. Katayama, T.; Chikamatsu, A.; Kamisaka, H.; Yokoyama, Y.; Hirata, Y.; Wadati, H.; Fukumura, T.; Hasegawa, T. Topotactic synthesis of strontium cobalt oxyhydride thin film with perovskite structure. *AIP Adv.* **2015**, *5*, 107147. [CrossRef]
18. Kawai, M.; Matsumoto, K.; Ichikawa, N.; Mizumaki, M.; Sakata, O.; Kawamura, N.; Kimura, S.; Shimakawa, Y. Orientation change of an infinite-layer structure $LaNiO_2$ epitaxial thin film by annealing with CaH_2. *Cryst. Growth Des.* **2010**, *10*, 2044–2046. [CrossRef]

19. Yajima, T.; Kitada, A.; Kobayashi, Y.; Sakaguchi, T.; Bouilly, G.; Kasahara, S.; Terashima, T.; Takano, M.; Kageyama, H. Epitaxial thin films of $ATiO_{3-x}H_x$ (A = Ba, Sr, Ca) with metallic conductivity. *J. Am. Chem. Soc.* **2012**, *134*, 8782–8785. [CrossRef]
20. Bouilly, G.; Yajima, T.; Terashima, T.; Kususe, Y.; Fujita, K.; Tassel, C.; Yamamoto, T.; Tanaka, K.; Kobayashi, Y.; Kageyama, H. Substrate-induced anion rearrangement in epitaxial thin films of $LaSrCoO_{4-x}H_x$. *CrystEngComm* **2014**, *16*, 9669–9674. [CrossRef]
21. Yamamoto, T.; Ohkubo, H.; Tassel, C.; Hayashi, N.; Kawasaki, S.; Okada, T.; Yagi, T.; Hester, J.; Avdeev, M.; Kobayashi, Y.; et al. Impact of lanthanoid substitution on the structural and physical properties of an infinite-layer iron oxide. *Inorg. Chem.* **2016**, *55*, 12093–12099. [CrossRef]
22. Patino, M.A.; Zeng, D.; Blundell, S.J.; McGrady, J.E.; Hayward, M.A. Extreme sensitivity of a topochemical reaction to cation substitution: $SrVO_2H$ versus $SrV_{1-x}Ti_xO_{1.5}H_{1.5}$. *Inorg. Chem.* **2018**, *57*, 2890–2898. [CrossRef] [PubMed]
23. Aschauer, U.; Pfenninger, R.; Selbach, S.M.; Grande, T.; Spaldin, N.A. Strain-controlled oxygen vacancy formation and ordering in $CaMnO_3$. *Phys. Rev. B* **2013**, *88*, 054111. [CrossRef]
24. Kutsuzawa, D.; Hirose, Y.; Chikamatsu, A.; Nakao, S.; Watahiki, Y.; Harayama, I.; Sekiba, D.; Hasegawa, T. Strain-enhanced topotactic hydrogen substitution for oxygen in $SrTiO_3$ epitaxial thin film. *Appl. Phys. Lett.* **2018**, *113*, 253104. [CrossRef]
25. Hayward, M.A.; Rosseinsky, M.J. Materials chemistry: Cool conditions for mobile ions. *Nature* **2007**, *450*, 960–961. [CrossRef]
26. Prado, F.; Mogni, L.; Cuello, G.J.; Caneiro, A. Neutron powder diffraction study at high temperature of the Ruddlesden-Popper phase $Sr_3Fe_2O_{6+\delta}$. *Solid State Ion.* **2007**, *178*, 77–82. [CrossRef]
27. Tang, Y.; Kobayashi, Y.; Shitara, K.; Konishi, A.; Kuwabara, A.; Nakashima, T.; Tassel, C.; Yamamoto, T.; Kageyama, H. On hydride diffusion in transition metal perovskite oxyhydrides investigated via deuterium exchange. *Chem. Mater.* **2017**, *29*, 8187–8194. [CrossRef]
28. Bither, T.A.; Prewitt, C.T.; Gillson, J.L.; Bierstedt, P.E.; Flippen, R.B.; Young, H.S. New transition metal dichalcogenides formed at high pressure. *Solid State Commun.* **1966**, *4*, 533–535. [CrossRef]
29. Bither, T.A.; Bouchard, R.J.; Cloud, W.H.; Donohue, P.C.; Siemons, W.J. Transition metal pyrite dichalcogenides. High-pressure synthesis and correlation of properties. *Inorg. Chem.* **1968**, *7*, 2208–2220. [CrossRef]
30. Martinolich, A.J.; Neilson, J.R. Toward Reaction-by-Design: Achieving Kinetic Control of Solid State Chemistry with Metathesis. *Chem. Mater.* **2017**, *29*, 479–489. [CrossRef]
31. Ni, J.; Gu, B. The metastable phase diagram and the kinetics of transient ordered states in a ternary system. *J. Phys. Condens. Matter* **1998**, *10*, 3523–3534. [CrossRef]